Digital Object Identifier (DOI): 10.1109/ECCE.2018.8557905

IEEE Energy Conversion Congress and Exposition (ECCE), Portland, OR, USA, 2018

Lifetime Control of Modular Smart Transformers Considering the Maintenance Schedule

Vivek Raveendran
Markus Andresen
Marco Liserre

Suggested Citation

V. Raveendran, M. Andresen and M. Liserre, "Lifetime Control of Modular Smart Transformers Considering the Maintenance Schedule," 2018 IEEE Energy Conversion Congress and Exposition (ECCE), Portland, OR, 2018, pp. 60-66.

Lifetime Control of Modular Smart Transformers Considering the Maintenance Schedule

Vivek Raveendran, Markus Andresen, Marco Liserre
Chair of Power Electronics, Faculty of Engineering
Christian-Albrechts-Universität zu Kiel, Kaiserstr. 2, 24143 Kiel, Germany
Email: vir@tf.uni-kiel.de, ma@tf.uni-kiel.de, ml@tf.uni-kiel.de

***Abstract*—Smart Transformers (ST) are power electronic transformers capable of providing grid services and DC connectivity compared to conventional low-frequency transformers. However, failure of the components and consequent maintenance is one of the major challenges compared to it's counterpart, limiting its application. By controlling the power flowing through the cells in a modular ST architecture, the remaining lifetime of these cells can be controlled. The idea is to schedule the maintenance by actively controlling the lifetime of the individual cells using an optimization algorithm. The proposed algorithm has the ability to schedule the maintenances according to predefined maintenance intervals. A potential ST architecture consisting of Cascaded H-bridge (CHB) and Dual-Active Bridge (DAB) converters are analyzed with simulations and experiments to validate the proposed power routing algorithm and its impact on the lifetime and maintenance scheduling.**

I. Introduction

With the changing world-view on renewable energy and environmental protection, the conventional power system network has been altered with higher share of renewable energy sources and electric vehicle charging stations. The ST is one promising solution to address the power flow flexibility while catering the requirements of changing grid scenarios [1], [2]. However, expected lower lifetime and consequent maintenance schedules are the key challenges of the ST compared to the conventional low-frequency transformer.

A modular architecture of ST combined with algorithms to control the power flow through the cells according to their aging is one of the promising solutions to increase the availability of ST [3]. The modular architecture offers several advantages such as the ability to route the power and provides redundancy. However, different cells can fail at different points in time leading to an increase in the maintenance schedules which may increase the maintenance costs, particularly when the ST is located in remote areas. Making use of the advantage of modularity, the power flow in each cell can be controlled to reduce the number of maintenance and can also predict the tentative maintenance schedules.

This paper proposes a lifetime control of modular ST comprising of CHB converter cells and DAB cells as shown in Fig. 1, using an optmization technique by considering the maintenance schedule. Using this approach, the frequency of maintenance can be reduced and moreover, the aging of the healthy cells are least affected, whereas the aging of the more aged cells are delayed.

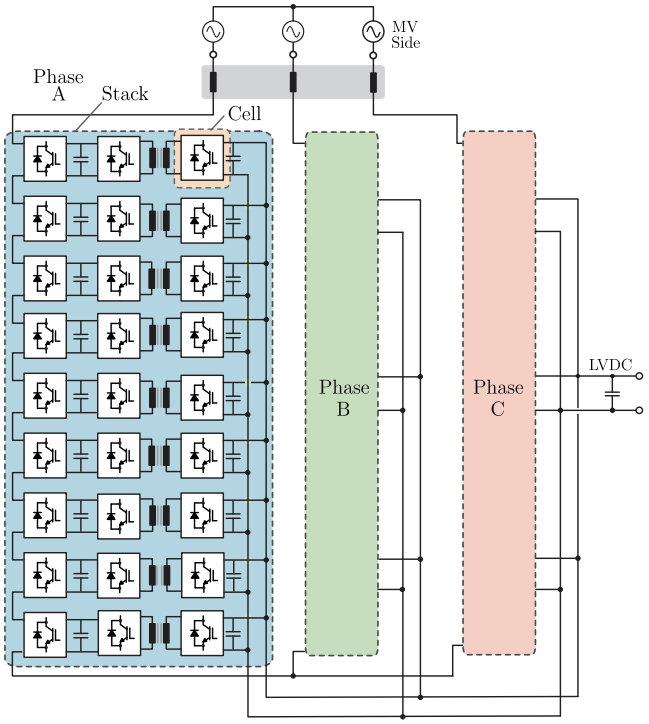

Fig. 1: ST architecture with CHB and DAB topologies.

The paper is organized as follows. The section II introduces the concept of power routing for maintenance scheduling and the development of the system model of the ST for lifetime studies is given in section III. The optimization algorithm for power routing is explained in section IV. The simulation results to show the effectiveness of the proposed power routing based on optimization algorithm are discussed in section V. The section VI shows the experimental validation of the proposed strategy and finally a conclusion is drawn in section VII.

II. Power Routing and Maintenance Scheduling

This section introduces the concept of power electronics reliability and explains the concept of power routing and the lifetime control through power routing for the maintenance scheduling of the ST.

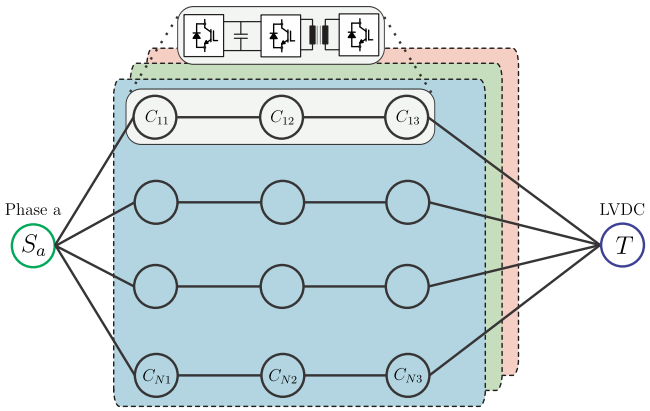

Fig. 2: Graph theory representation of ST illustrating the power paths.

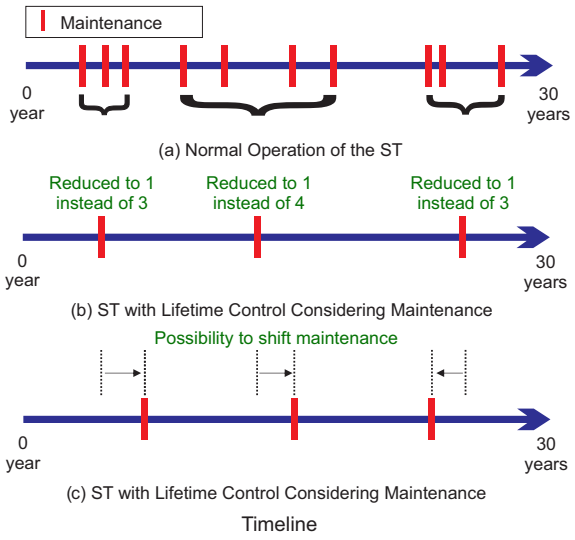

Fig. 3: Impact of proposed algorithm on the maintenance scheduling of modular ST (a) Without proposed algorithm (b) With proposed algorithm (c) Demonstrating the flexibility of shifting maintenance

A. Wear-out based Power Electronics Reliability

The processed power determines the junction temperature variations in the power modules. The junction temperature swings influence the aging and deterioration of the power modules given by (1).

$$N_f = a_1(\Delta T)^{a_2} \cdot e^{\frac{a_3}{T_{j,av}+273°C}} \tag{1}$$

where, N_f is the number of thermal cycles to failure , ΔT is the temperature swing, $T_{j,av}$ represents average junction temperature and a_1, a_2 and a_3 are the device dependent coefficients. [4]. Subsequently, Miner's rule can be applied to calculate the accumulated damage given by [5]

$$D = \sum \frac{N_i}{N_{fi}} \tag{2}$$

where D is the accumulated damage, N_i the number of cycles and N_{fi} the durability of the i-th stress range. The device reaches end of life when the accumulated damage becomes 1.

B. Concept of Power Routing and Lifetime Based Maintenance Scheduling

Reliability and availability of the ST is one of the key challenges compared to the conventional low-frequency transformer with very high expected lifetimes. According to the well-known bathtub curve for reliability, during the useful life of the device, failures are classified into random failures and wear-out based failures [6]. The junction temperature thermal cycling is the main cause of wear-out based failures whereas random failures can be due to cosmic rays, lightning etc. It is logical to assume that in the ST with many converter cells, the cells have different aging due to random failures or unsymmetrical wear-out [2].

Consequently, the ST is composed of cells with different ages and they can fail at different times leading to numerous maintenance schedules. The idea of power routing is to actively control the loading of cells to influence their junction temperature and thereby the lifetime. The power flow paths in the ST architecture given in Fig. 1 is represented using graph theory in Fig. 2. The graph theory representation provides the overview of the power flow paths from MVAC to LVDC. Each power flow path consist of a CHB cell connected to a DAB cell processing the same power.

Fig. 3 shows the graphical representation of the effect of controlling the maintenance schedule on a modular system like the ST. Without any lifetime control, the individual units fail at different points in time resulting in higher number of maintenance schedules as depicted in Fig. 3(a). With active control of the lifetime considering the maintenance schedules, the number of maintenances can be reduced as illustrated in Fig. 3(b).

III. System Modeling for Lifetime Analysis

The detailed modeling for lifetime study is elaborated in this section. The modeling forms the basis for validating the proposed algorithm.

A. Methodology of Reliability/Lifetime Study

The methodology of lifetime estimation and lifetime control is summarized in Fig. 4. In order to analyze the lifetime using the thermal stress analysis, a mission profile is used to generate the working condition of the power converter. Depending on the mission profile, the thermal loading of the converter is obtained using an electro-thermal model of the system. Once the junction temperature fluctuations are known, the lifetime can be calculated using the rainflow counting method and a lifetime model of the power device.

B. Device modeling

The semiconductor module from Danfoss DP25H1200T101616 is characterized in the laboratory

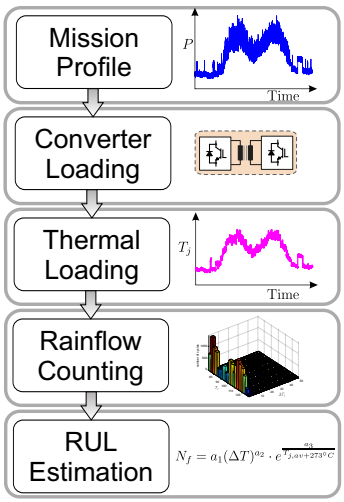

Fig. 4: Functional block diagram for the lifetime analysis.

to obtain the switching energy vs collector current (E_{on} & E_{off} vs I_c) characteristics and the on-state voltage vs collector current characteristic for obtaining conduction losses (V_{ce} vs I_c). The conduction losses of the diode is characterized with forward voltage drop vs device current(V_f vs I_c). The device loss curves for conduction and switching losses are curve fitted to obtain an approximation as given in

$$\begin{bmatrix} E_{on} \\ E_{off} \\ V_{ce} \\ V_f \end{bmatrix} = \begin{bmatrix} a_1 & b_1 & c_1 \\ a_2 & b_2 & c_2 \\ a_3 & b_3 & c_3 \\ a_4 & b_4 & c_4 \end{bmatrix} \begin{bmatrix} I_c^2 \\ I_c \\ 1 \end{bmatrix} \tag{3}$$

Parameter	a_i	b_i	c_i
E_{on}	6.8×10^{-6}	1.1×10^{-5}	1.6×10^{-4}
E_{off}	1.2×10^{-8}	7.0×10^{-5}	1.8×10^{-5}
V_{ce}	-0.0025	0.13	0.75
V_f	-6.3×10^{-4}	0.046	0.86

TABLE I: Device parameter curve fitting values

The Table I provides the values of curve fitting constants a_i, b_i and c_i, where $i \in \{1,2,3,4\}$. The device tests are carried out at an ambient temperature of $25^\circ C$. With instantaneous device current, switching and conduction losses of the devices are computed using (3).

C. Development of ST Model for Lifetime Analysis

In order to test the proposed lifetime control, an electro-thermal model of the system has been modeled. The ST parameters are given in Table II.

Rated Power	**MVAC**	**LVAC**	**Grid frequency**	**LVDC**
1 MVA	10 kV	$400V$	$50Hz$	$800V$

TABLE II: ST specification.

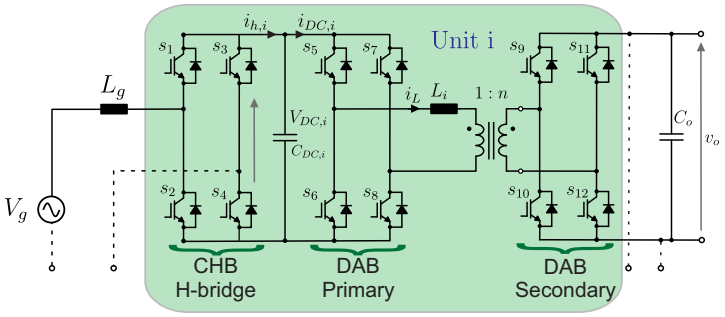

Fig. 5: ST architecture with CHB and DAB topologies.

CHB modeling for lifetime analysis: The Fig. 5 shows the detailed schematic of one power flow path of the ST comprising of CHB and DAB converters. The CHB is described by the electrical equations given by [7].

$$L_g \frac{di_L}{dt} = \sum_{i=1}^{N} (m_i) v_{DC,i} - v_g \tag{4}$$

where m_i is the modulation index of each H-bridge.

$$C_{DC,i} \frac{dv_{DC,i}}{dt} = i_{h,i} - i_{DC,i} \tag{5}$$

The grid current i_g flows through the IGBT (i_c) or the diode (i_d) depending on the direction of i_g. The conduction loss of IGBT at any instant is given by

$$P_{cond,IGBT} = V_{ce} i_c \cdot \frac{1}{2}(1 + m_i(sin(\omega t + \phi))) \tag{6}$$

The conduction loss of the anti-parallel diode at any instant is given by

$$P_{cond,diode} = V_f i_d \cdot \frac{1}{2}(1 - m_i(sin(\omega t + \phi))) \tag{7}$$

The conduction and switching losses are calculated according to the mission profile as input.

DAB modeling for lifetime analysis: Considering phase shift modulation for DAB cell i, the power handled is given by

$$P_i = \frac{m_{DAB,i} V_{DC,i}^2 D_i (1 - D_i) T_{sw,DAB}}{2L_i} \tag{8}$$

where P_i is the power processed by DAB cell i, $m_{DAB,i}$ is the modulation index of the cell DAB_i, $V_{DC,i}$ is the MVDC link voltage, L_i is the leakage inductance and $T_{sw,DAB}$ is the switching time period. Depending on the operating power, duty cycle D_i is calculated and subsequently the primary $i_{prim,i}$ and secondary currents $i_{sec,i}$ through the switches are also calculated. Finally, the switching and conduction losses are calculated from current values and device parameters. [8].

Thermal network modeling: The thermal model consists of the thermal impedance of junction to case, case to heatsink and heatsink to ambient represented by a Foster network. The junction temperature T_j of the device (IGBT and diode) can be calculated from the equivalent impedance of the Foster network and the total losses in the device as given by (9)

$$T_j(t) = Z_{th,j-a} P_{tot}(t) + T_a(t) \tag{9}$$

where $Z_{th,j-a}$ is the equivalent impedance of the Foster network, P_{tot} is the total losses in the device, T_a is the ambient temperature.

IV. Algorithm for Adaptive Lifetime Control

This section describes the proposed algorithm for adaptive lifetime control to schedule the maintenance of the ST. The ST is composed of many converter cells which have embedded junction temperature sensing of the power devices through the measurement of collector emitter voltage [9]. By knowing the junction temperature profile of the devices, the accumulated damage, D, can be calculated using the method described in Section II.

The idea is to control the lifetime of the power semiconductor devices by actively controlling the power flow through them. The proposed algorithm uses optimization to define the power flow through each of the cell depending on the aging of the cell. The algorithm is shown graphically in Fig. 6. The thermal cycling causes the aging of the power modules and the accumulated damage, D, can be calculated using the method described in Section II. In this method, the mission profile for the past week is used to calculate the incremental accumulated damage, ΔD, for each cell.

Subsequently, the total accumulated damage can be calculated for each converter over m weeks using (10)

$$D_i = D_{ini,i} + \sum_{period=1}^{m} \Delta D_i \tag{10}$$

where D_i is the total accumulated damage of converter cell i and $D_{ini,i}$ is the initial damage. ΔD_i is the rate of change of damage for the past week.

The expected Remaining Useful Lifetime (RUL) ($LT_{exp,i}$) at every control interval can be calculated as follows

$$LT_{exp,i} = \frac{1 - D_i}{\Delta D_i} \tag{11}$$

The required number of maintenances are defined by maintenance interval factor λ. For example, considering an ST with a required lifetime of 30 years and 3 maintenance schedules, the maintenance intervals can be defined as

$$\lambda_1 = [0,10]\,\text{years},\ \lambda_2 = [10,20]\,\text{years},\ \lambda_3 = [20,30]\,\text{years}.$$

The cells with $LT_{exp,i}$ in the maintenance intervals λ_i are grouped together and the objective of the algorithm is to converge the failures of these cells in the specified maintenance intervals. Consequently, a weight is assigned to each converter in a group to determine the power flow, and thereby control the lifetime. The weight for each cell in group is formulated as

$$W_i = K_D \left(\frac{\sum_{i=1}^{k} LT_{exp,i}}{k} - LT_{exp,i} \right) \tag{12}$$

where K_D is a proportional constant which is a function of individual accumulated damages of each cell, D_i, and k is the number of cells in a group belonging to maintenance interval λ_i.

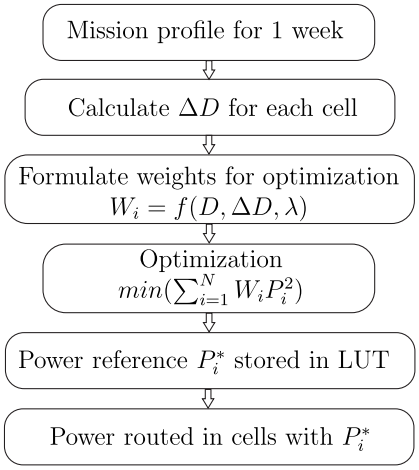

Fig. 6: Graphical representation of lifetime control algorithm

Finally, the weights are given to an optimization algorithm using a convex optimization function as given in (13)

$$min(\sum_{i=1}^{N} W_i P_i^2) \tag{13}$$

subjected to the constraints

$$\sum_{i=1}^{N} P_i = P \ \ \& \ \ 0 \geq P_i \leq \frac{P}{N} \tag{14}$$

where W_i is the weight for each cell, P_i, the power processed by each cell, P is the total power and N is the total number of cells.

The constraints are imposed on the converters in such a way that the power routing is active in partial load operation, whereas all process equal power when the system is at full load. Most of the time, the system is not operating with full load, which enables to route the power unequally. This means the converters need not to be over-sized for this strategy.

The optimization algorithm determines the power references P_i^* for each converter cell for the entire operating range of the system, $P = [0,1]\,p.u$ and are stored in a look-up table. The offline method saves the online computation effort for the generation of optimal power reference at each system operating point.

V. Simulation Results

In order to evaluate the effectiveness of the proposed algorithm, simulations studies are conducted with the electro-thermal model developed in Section III. First, the effect of parameter variations of the lifetime model on the lifetime estimation is validated through Monte Carlo simulations. A study case is presented for an ST with 10 CHB and DAB cells for normal operation and with the proposed algorithm.

Effect of Parameter Variation on Lifetime Estimation: The measured junction temperature of the power modules are used to calculate the remaining useful lifetime (RUL) using (1).

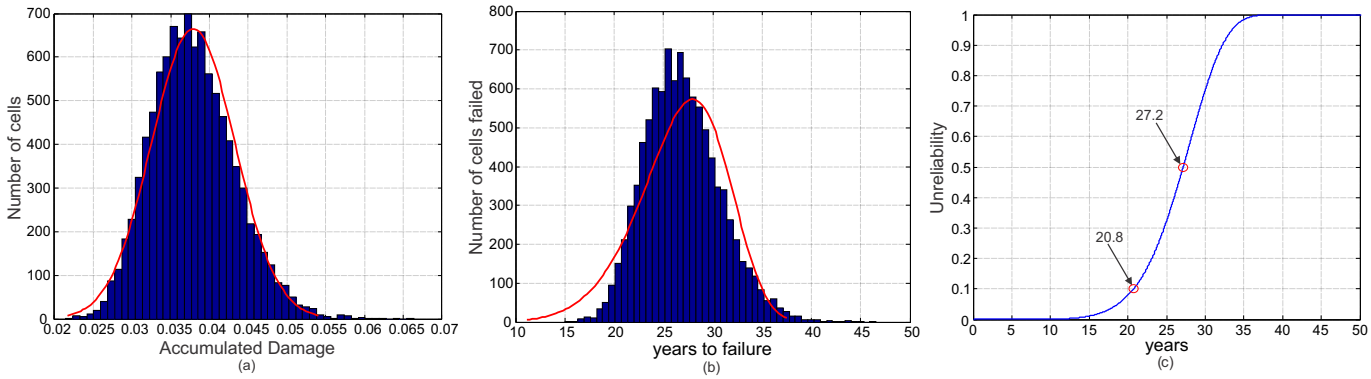

Fig. 7: Monte Carlo analysis considering the parameter variations of lifetime model (a) Annual accumulated damage (b) Time to failure (c) Unreliability

The device dependent parameters a_1, a_2 and a_3 are curve fitted values form power cycling tests [4]. These parameters can be represented by normal distribution function assuming a variation of 5%. For sensitivity analysis considering these parameter variations, Monte-Carlo simulation for 10000 samples is done using the system model developed in section II and the results are shown in Fig 7(a)-(c). The annual accumulated damage from the Monte Carlo simulations is shown in Fig 7(a). Fig 7(b) shows the estimated lifetime of the samples which can be approximated by a Weibull distribution. Subsequently, unreliability or cumulative percentage of failure can be calculated using the Weibull distribution parameters as in Fig 7(c) and can be noted that the 10% of total cells are predicted to fail at 21 years and 50% at 27 years. For the lifetime control algorithm, lifetime at 10% probability of failure is taken to incorporate the effect of probabilistic nature of failure.

Comparison of aging of cells of ST with and without lifetime control: A system with 10 DAB cells connected to CHB cells is considered here with each cell having different initial accumulated damage. The electro-thermal model of the ST is fed with different mission profiles reflecting the grid conditions [10]. The progression of accumulated damage over time for the normal operation of the ST is shown in Fig. 8. Here, only the failure of DAB cells are shown since the effect of power routing algorithm on CHB is limited [11].

Without any lifetime control, the cells fail at different instants in time, leading to many maintenance schedules. Fig. 9 shows the probability of failure of the system with the assumption that the cells are replaced at 10% probability of failure. The probability of failure of the ST shows that there is a high chance of failure in the system spread over years, which can significantly affect the availability of the ST.

With the proposed algorithm, the accumulated damage, D_i, of each cell converges in such a way that the number of maintenance schedules is reduced while the decrease in the lifetime of the healthy cells is minimal. In this case, 3 maintenances are selected with the maintenance intervals given

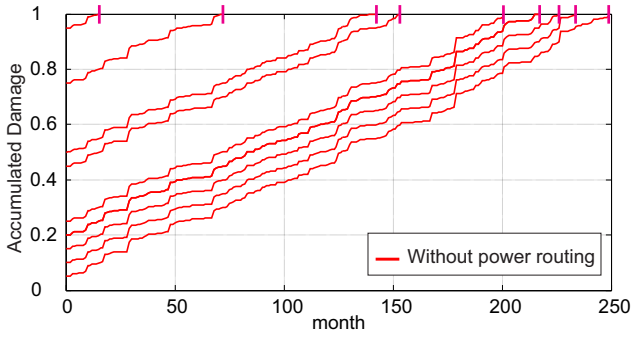

Fig. 8: Progression of accumulated damage vs. time of the ST for normal operation

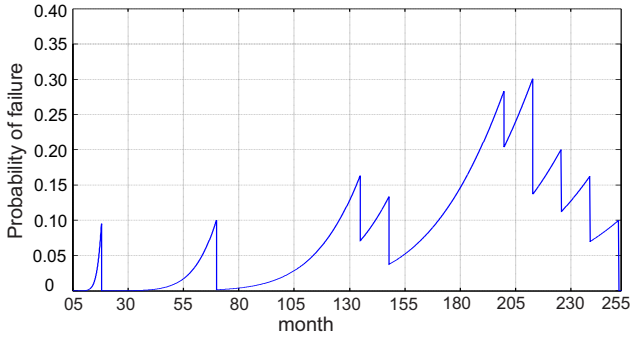

Fig. 9: Probability of failure of any cell of the ST for normal operation

as

$$\lambda_1 = [0, 96],\ \lambda_2 = [96, 192],\ \lambda_3 = [192, 288]\,\text{months}.$$

The cells in the the maintenance intervals are grouped together and the weights of the optimization (13) are formulated to converge the failures of these cells. The effectiveness of the method is illustrated in Fig. 10 and Fig. 11. Fig. 10 shows the progression of accumulated damages of the cells with lifetime control. The accumulated damages of the selected cells in the three maintenance intervals effectively converge to 3 maintenance schedules. The probability of failure of the system for the proposed algorithm is depicted in Fig. 11. Compared to

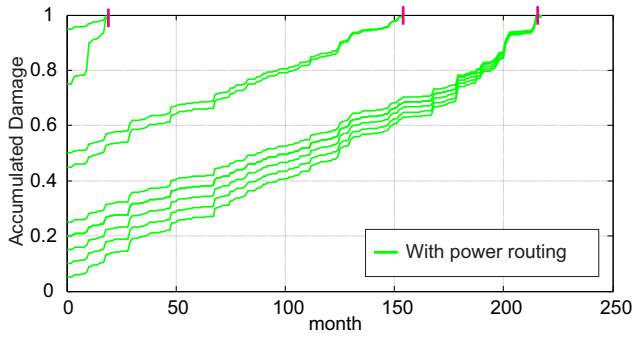

Fig. 10: Progression of accumulated damage vs. time of the ST with lifetime control

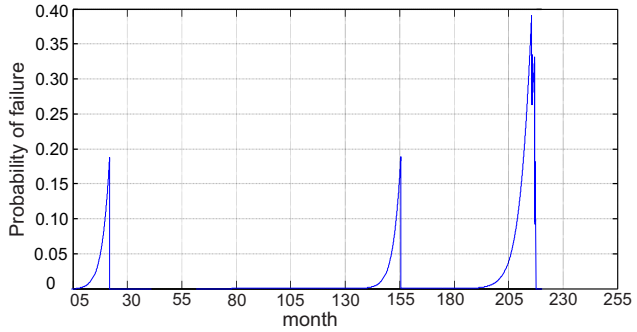

Fig. 11: Probability of failure of any module of the ST with lifetime control

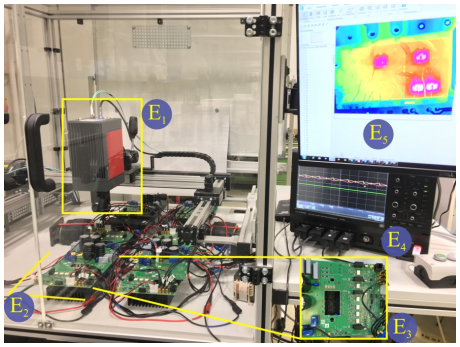

Fig. 12: The experimental setup showing 5-level CHB connected to 2 DABs (E_2) with open IGBT modules (E_3) and high resolution IR camera (E_1).

the failure probability without lifetime control, the proposed algorithm demonstrates a concentrated probability of failure around 3 maintenance instants. Therefore, the risk of failure of the ST is reduced compared to the operation with balanced power.

VI. Experimental Validation

The industry practices and literature extracts the lifetime of the power devices from the thermal cycling tests [4], [12]. In order to validate the lifetime control of ST, the capability of the experimental setup to route the power unequally to control the junction temperature is demonstrated in this section.

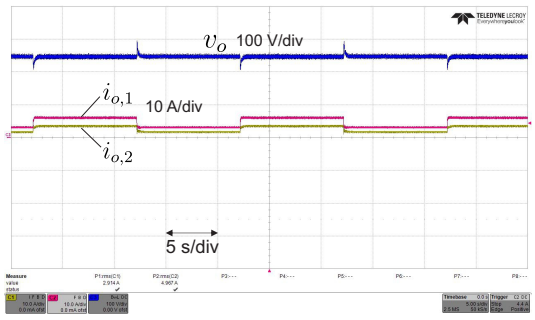

Fig. 13: The output currents of both DABs $(i_{o,1-2})$and the load voltage $(v_o)$for unbalanced power distribution for the given mission profile.

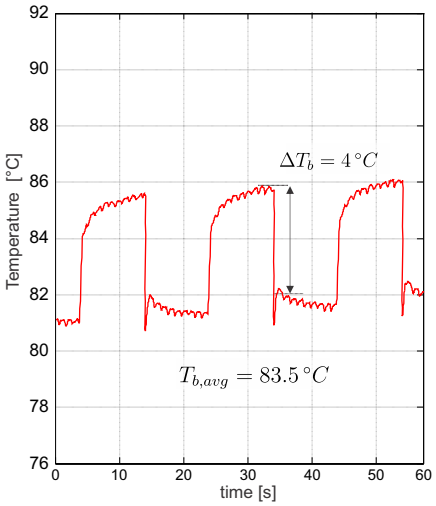

Fig. 14: Junction temperature profile of DAB cells with balanced power sharing

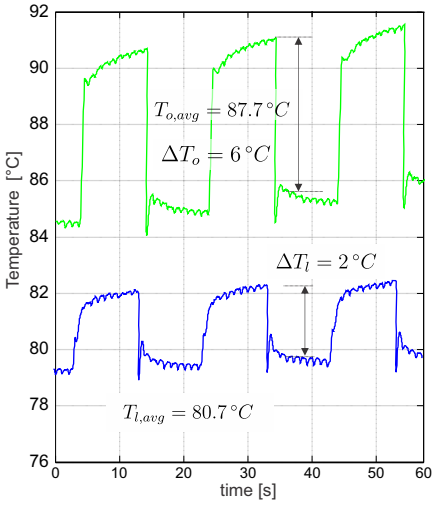

Fig. 15: Junction temperature profile of DAB cells with power routing

To demonstrate the proposed power routing control strategy, a small scale prototype of a five level CHB connected to two DABs has been developed as illustrated in Fig. 12. The

H-bridges of CHB and DAB are made with open-module DP25H1200T101616 from Danfoss to facilitate direct junction temperature measurements. The setup is controlled by the dSPACE SCALEXIO system. The experimental setup parameters are summarized in Table III.

Symbol	Description	Value
V_g (rms)	Grid voltage (rms)	$230V,\ 50Hz$
L_g	Filter inductance (MV side)	$3.8mH$
$V_{DC,1} = V_{DC,2}$	DC-link voltage reference	$250V$
V_0	DC-link voltage (LV side)	$250V$
n	MFT turn ratio	$1:1$
$f_{sw,CHB}$	Switching frequency of the CHB	$3kHz$
$f_{sw,DAB}$	Switching frequency of the DAB	$12kHz$

TABLE III: Experimental setup parameters

Here, a mission profile with a step change from $P_n = 1.2\,kW$ to $P_n = 2.4\,kW$ with each power cycle lasting for $10\,s$ is applied for validation. When the power routing is not activated, the DABs share the power equally. With power routing control active, the CHB cell 1 and DAB,1 process $\approx 70\%$ more power than the CHB cell 2 and DAB,2 as shown in Fig. 13. The Fig. 13 shows the output currents of DABs for an unbalanced power distribution for a step change in the output power. The DAB output voltage V_o is maintained constant by the controller during the power steps showing the robustness of the ST controller.

The Fig. 14 and 15 shows the impact on the junction temperature of the ST DAB cells without and with lifetime control respectively. In the balanced power sharing case, the thermal swing is $\Delta T_b = 4°C$ with each DAB delivering $1.25kW$. Fig. 15 shows the thermal cycling for overloaded and lightly loaded cells with $\Delta T_0 = 6°C$ and $\Delta T_l = 2°C$ when delivering power $P_1 = 1.5\,kW$ and $P_2 = 1\,kW$ respectively. Therefore, by adjusting the power sharing between the cells, their junction temperatures can be influenced in order to control the lifetime. This demonstrates the proof of concept of the power routing lifetime control strategy.

VII. Conclusion

The lifetime control of the modular ST using optimization algorithm by considering the maintenance schedule is presented in this paper. To validate the impact of the proposed lifetime control strategy, an electro-thermal model of the ST is developed for lifetime analysis. The simulation results demonstrate the effectiveness of the proposed algorithm to synchronize the failures of the cells with maintenance of the ST and thereby decreasing the maintenance schedules from 10 to 3 times. Moreover, the proposed method reduces the probability of failure of the ST over the time by concentrating the failures around the maintenance period. For the experimental proof of concept, a small-scale prototype of ST with CHB and DAB with open IGBT modules for junction temperature measurement is used. The junction temperature profile of the ST cells with and without the lifetime control algorithm demonstrates the ability of the controller to influence the thermal cycling, and consequently the lifetime of the cells.

Acknowledgment

This work was supported by the European Research Council under the European Unions Seventh Framework Programme (FP/2007-2013) / ERC Grant Agreement n. 616344-HEART.

References

[1] A. Q. Huang, "Medium-voltage solid-state transformer: Technology for a smarter and resilient grid," *IEEE Industrial Electronics Magazine*, vol. 10, no. 3, pp. 29–42, Sept 2016.

[2] M. Liserre, M. Andresen, L. Costa, and G. Buticchi, "Power routing in modular smart transformers: Active thermal control through uneven loading of cells," *IEEE Industrial Electronics Magazine*, vol. 10, no. 3, pp. 43–53, Sept 2016.

[3] M. Andresen, V. Raveendran, G. Buticchi, and M. Liserre, "Lifetime-based power routing in parallel converters for smart transformer application," *IEEE Transactions on Industrial Electronics*, vol. PP, no. 99, pp. 1–1, 2017.

[4] M. Held, P. Jacob, G. Nicoletti, P. Scacco, and M. H. Poech, "Fast power cycling test of igbt modules in traction application," in *Proceedings of Second International Conference on Power Electronics and Drive Systems*, vol. 1, May 1997, pp. 425–430 vol.1.

[5] D. R. Jones and M. F. Ashby, *Engineering materials 1: An introduction to properties, applications and design*. Elsevier, 2011.

[6] P. O'Connor and A. Kleyner, *Practical reliability engineering*. John Wiley & Sons, 2012.

[7] J. Rodriguez, J.-S. Lai, and F. Z. Peng, "Multilevel inverters: a survey of topologies, controls, and applications," *IEEE Transactions on Industrial Electronics*, vol. 49, no. 4, pp. 724–738, Aug 2002.

[8] A. K. Jain and R. Ayyanar, "Pwm control of dual active bridge: Comprehensive analysis and experimental verification," *IEEE Transactions on Power Electronics*, vol. 26, no. 4, pp. 1215–1227, April 2011.

[9] P. Asimakopoulos, K. D. Papastergiou, T. Thiringer, M. Bongiorno, and G. L. Godec, "On vce method: in-situ temperature estimation and aging detection of high-current igbt modules used in magnet power supplies for particle accelerators," *IEEE Transactions on Industrial Electronics*, pp. 1–1, 2018.

[10] M. Pignati, M. Popovic, S. Barreto, R. Cherkaoui, G. D. Flores, J. Y. L. Boudec, M. Mohiuddin, M. Paolone, P. Romano, S. Sarri, T. Tesfay, D. C. Tomozei, and L. Zanni, "Real-time state estimation of the epfl-campus medium-voltage grid by using pmus," in *2015 IEEE Power Energy Society Innovative Smart Grid Technologies Conference (ISGT)*, Feb 2015, pp. 1–5.

[11] V. Raveendran, M. Andresen, M. Liserre, and G. Buticchi, "Lifetime-based power routing of smart transformer with chb and dab converters," in *2018 IEEE Applied Power Electronics Conference and Exposition (APEC)*, March 2018, pp. 3523–3529.

[12] D. Zhou, H. Wang, F. Blaabjerg, S. K. Koer, and D. Blom-Hansen, "System-level reliability assessment of power stage in fuel cell application," in *2016 IEEE Energy Conversion Congress and Exposition (ECCE)*, Sept 2016, pp. 1–8.